Development of new ganglioside probes and unraveling of raft domain structure by single-molecule imaging

Development of new ganglioside probes and unraveling of raft domain structure by single-molecule imaging

Kenichi G. N. Suzuki[1,2,3*], Hiromune Ando[1,2*], Naoko Komura[1,2], Takahiro Fujiwara[2], Makoto Kiso[2], Akihiro Kusumi[2,4]

[1]Center for Highly Advanced Integration of Nano and Life Sciences (G-CHAIN), Gifu University, Gifu 501-1193, Japan. [2]Institute for Integrated Cell-Material Sciences (WPI-iCeMS), Kyoto University, Kyoto 606-8507, Japan. [3]The Institute for Stem Cell Biology and Regenerative Medicine (inStem), The National Centre for Biological Sciences (NCBS), Bangalore, 650056, India. [4]Membrane Cooperativity Unit, Okinawa Institute of Science and Technology, Onna-son, Okinawa 904-0412, Japan.

*Co-corresponding authors:

Kenichi G. N. Suzuki
Center for Highly Advanced Integration of Nano and Life Sciences (G-CHAIN), Gifu University, Gifu 501-1193, Japan.
Ph: +81-58-293-3330
Email:kgsuzuki@gifu-u.ac.jp

Hiromune Ando
Center for Highly Advanced Integration of Nano and Life Sciences (G-CHAIN), Gifu University, Gifu 501-1193, Japan.
Ph: +81-58-293-3452
Email:hando@gifu-u.ac.jp

Abstract

Gangliosides are involved in a variety of biological roles and are a component of lipid rafts found in cell plasma membranes (PMs). Gangliosides are especially abundant in neuronal PMs and are essential to their physiological functions. However, the dynamic behaviors of gangliosides have not been investigated in living cells due to a lack of fluorescent probes that behave like their parental molecules. We have recently developed, using an entirely chemical method, four new ganglioside probes (GM1, GM2, GM3, and GD1b) that act similarly to their parental molecules in terms of raft partitioning and binding affinity. Using single fluorescent-molecule imaging, we have found that ganglioside probes dynamically enter and leave rafts featuring CD59, a GPI-anchored protein. This occurs both before and after stimulation. The residency time of our ganglioside probes in rafts with CD59 oligomers was 48 ms, after stimulation. The residency times in CD59 homodimer and monomer rafts were 40 ms and 12 ms, respectively. In this review, we introduce an entirely chemical-based ganglioside analog synthesis method and describe its application in single-molecule imaging and for the study of the dynamic behavior of gangliosides in cell PMs. Finally, we discuss how raft domains are formed, both before and after receptor engagement.

1. Introduction

Gangliosides are glycosphingolipids containing one or more sialic acid (N-acetyl-neuraminic acid) groups. They are particularly abundant in neuronal cell plasma membranes (PMs) [1, 2]. More than 40 types of ganglioside have been described, with the location and number of sialic acids groups present being different in each. Gangliosides containing one, two, three, or four sialic acid groups are termed GM, GD, GT, and GQ, respectively. Gangliosides are further defined using numbers to indicate their migratory position after thin-layer chromatography (e.g., GQ1b, GM3, GD3). Gangliosides are known to have a variety of important physiological functions in cell PMs (Fig. 1). For example, they are involved in the invasion of microbial toxins [3], viruses [4, 5], and bacteria into cells. They have also been shown to regulate membrane receptor activity [6]. More specifically, previous studies have indicated that GM3 inhibits activation of epidermal growth factor receptors (EGFRs) [7-11]. It has also been reported that activation of the nerve growth factor (NGF) receptors (Trk) is enhanced by interactions with GM1 [12, 13]. The ganglioside GD3 was found to enhance adhesion signaling by recruiting integrins to lipid rafts [14] and GQ1b was found to increase tyrosine phosphorylation of N-methyl-d-aspartate (NMDA) subunit 2B, which may subsequently enhance NMDA receptor synaptic activation [15]. Finally, gangliosides are known to be involved in various infections and the onset of several diseases, such as Guillain-Barre syndrome [16-21], Alzheimer's disease [22-25], and gangliosidosis [26-29].

Through certain interactions with cholesterol, gangliosides are also known to be involved in the formation of raft domains found in PMs [30-33].

Interestingly, these lipid rafts facilitate the regulatory effects that gangliosides have on receptor activity. For example, inhibition of EGFR activity by GM3 in giant unilamellar vesicles (GUVs) is more effective in the presence of liquid ordered (Lo) phase regions (raft-like domains) [11].

However, gangliosides have not directly been observed in the PMs of living cells and previous studies have been performed using fixed PMs or by examining how the expression levels of gangliosides affect receptor activities and other cellular processes. This is primarily due to the scarcity of fluorescent ganglioside probes that behave in a similar manner to the parental molecules. Although GM1 analogs have been synthesized that possess alkyl chains or glycans bound to fluorophores [34-39], these analogs do not partition into the raft-like domains [40]. They also do not bind proteins as strongly as their parental ganglioside molecules [38]. To overcome these issues, ganglioside-binding proteins, such as cholera toxin subunit B (CTB), are often used to examine the location of gangliosides in cells [41-47]. However, these proteins are multivalent and can crosslink gangliosides, changing their lateral distribution in the PMs of cells [48-51]. Even if PMs are fixed using 4% paraformaldehyde and 0.5% glutaraldehyde, a significant fraction of lipid molecules are still mobile [52, 53] and can crosslink ganglioside molecules. Similarly, it is difficult to perform immunohistochemical staining of gangliosides as labeling using primary and secondary antibodies also results in crosslinking, even after cell fixation. This leads to the creation of bright fluorescent patches of gangliosides [52, 53]. Due to all of these various factors, it has been extremely difficult to examine the lateral distribution of gangliosides in cell PMs.

To address this issue, we have used entirely chemical methods [54-60] to develop fluorescent ganglioside probes that behave in a similar manner to their parental gangliosides [61]. In this review, we provide an overview of the studies performed to elucidate the dynamic behaviors of gangliosides in cell PMs. We also introduce some of the uses of our new fluorescent probes, such as single-molecule imaging and understanding how raft domains are formed, both before and after receptor engagement.

1.1. Synthesis of ganglioside probes

As previously described, the synthesis of fluorescently labeled ganglioside analogs has been reported by many research groups, primarily GM1. An important factor when synthesizing fluorescent analogs of gangliosides is that the chemically labile fluorescent dye should be incorporated at a specific position in the target molecule. Consequently, dye incorporation must be chemo-selectively executed at the final step of synthesis. However, this means that the final incorporation will be in the presence of an array of hydroxyl groups. To meet this synthetic limitation, a highly reactive functional group needs to be incorporated into the ganglioside molecule to act as a specific coupling partner for the fluorescent dye reagent. One such method is based on exploiting the endogenous amido moieties of sialic acid and ceramide, typically found in gangliosides. These two groups are readily converted into free amino groups by basic hydrolysis to produce 5-amino-sialic acid and 2-amino-sphingosine containing gangliosides, respectively [62]. Several research groups have used this approach to successfully incorporate fluorescent dyes at the C5-amino group of sialic acid

and/or the C2-amino group of sphingosine (Fig. 2a) [35-37, 63].

In addition, Wilchek *et al.* (1980) developed a selective conversion method that changed the glycerol chain of sialic acid into a C7-aldehyde derivative [64]. Through taking advantage of the high electrophilicity of this aldehyde group, C7-aldehyde gangliosides were able to be conjugated to various amine-terminated fluorophores (Fig. 2b) [38]. These approaches are described as break-down (or top-down) methods as they utilize gangliosides isolated from natural sources as the starting materials (in almost all cases, these are bovine brain matter). However, these methods produce heterogeneous mixtures of fluorescent analogs that differ in their chain length due to different sphingosine moieties.

Alternatively, Rich *et al.* (2011) showcased *de-novo* (bottom-up) synthesis of homogenous fluorescent ganglioside GM3 using a chemoenzymatic method that utilized glycoside hydrolase mutants described as glycosynthases [65]. This approach was shown to be tolerant to modified glycosyl donors and was suitable for the construction of a C9-azido-lyso-GM3 variant. This underwent subsequent chemoselective conjugation with fluorescent dyes, creating a GM3 molecule with dual fluorescence (Fig. 3) [66].

More recently, we have developed novel fluorescent ganglioside probes that are useful for studying interactions between lipid rafts and gangliosides in PMs using a *de-novo* chemical synthesis method (Fig. 4) [61]. When designing these fluorescent gangliosides, we paid particular consideration to the importance of the ceramide (Cer) moiety in the interactions with other membrane lipids and cholesterols in the inner and outer leaflets of PMs [67, 68]. By taking this into account, we aimed to incorporate fluorescent dyes using the glycan moiety found

in gangliosides. To modify linear ganglioside GM3, one of five dyes was attached to the central position (position C6 of the inner galactose (Gal) of GM3; position G6) and the outermost position (position C9 of sialic acid; position S9). The effects of the dye on the physical properties of the ganglioside were examined in relation to a preference to incorporate into lipid rafts, referred to as 'raftphilicity'. For GM1, GM2, and GD1b with branched glycans, the outermost positions (positions S9 and/or C6 of the terminal sugar residue) were modified with a dye.

To ultimately realize our fluorescent ganglioside design, we applied our previously developed method to the synthesis of gangliosides. This system uses a glucosyl ceramide (Glc-Cer) cassette [56, 58-60] and *N*-Troc-sialyl galactose (Neu5Troc-Gal) [54, 69] as the key synthetic units. Neu5Troc-Gal unit **1** (Fig. 5) was used as a platform for modifying Neu and Gal moieties with amine-relevant substituents to couple the fluorescent dye.

1.1.1. Synthesis of fluorescent GM3 analogs

Following previously published reports, disaccharide unit **1** was converted into a 4,6-diol derivative and further modified with an azide group at the C6 position to give a C6-azido derivative (Fig. 5). Subsequent conversion with a trichloroacetimidate donor gave **2** that was used for the synthesis of the G6 analogs. For the synthesis of the S9 analogs, the sialic acid moiety of **1** was transformed into an *N*-acetyl tetraol. An azide group was then incorporated at the C9 position in a similar manner to that for compound **2**. Next, the azide group was converted into a trifluoroacetamide (NHTFAc) group, to give compound **3**. The protecting groups were manipulated to produce the C9-NHTFAc-Neu-Gal

donor **4**. Neu-Gal donors (**2** and **4**) and the Glc-Cer acceptor **5** were glycosylated, providing high yields of the two ganglioside GM3 frameworks **6** and **7**. Following global deprotection of **6**, the azide was reduced to an amine and reacted with the activated ester of a fluorescent dye to create the G6 GM3 analogs (TMR-G6-GM3 and 594-G6-GM3). In contrast, **7** was converted to a corresponding amino-GM3 precursor via removal of the *p*-methoxybenzyl protecting groups and subsequent hydrolysis. The fluorescent group was then incorporated at position C9 of the sialic acid group to create the S9 GM3 probes (TMR-S9-GM3, Fl-S9-GM3, 594-S9-GM3, 647N-S9-GM3, and 488-S9-GM3) [61].

1.1.2. Synthesis of fluorescent GM1 analogs

The synthetic methodology used to create the GM3 analogs was applied to the more complex GM1 analogs that contained branched glycan moieties (Fig. 6). For the synthesis of the S9 GM1 core sequence, C9-NHTFAc Neu-Gal **3** was converted into the corresponding glycosyl acceptor **8** via selective protection of the hydroxyl groups. Next, **8** was elongated using the disaccharide donor **9** via a stereoselective glycosylation reaction [70] to create a branched tetrasaccharide. This tetrasaccharide was converted into a glycosyl imidate donor through an eight-step manipulation of protecting groups to create **10**. In contrast, the synthesis of the termG6 GM1 core sequence began with the glycosylation of branched trisaccharyl acceptor **11** (previously developed in our group) [59] with C6-NHTFAc galacotosyl imidate **12**. This resulted in a 92% tetrasaccharide yield. Following a procedure similar to that used for the S9 probes, the tetrasaccharide was converted to donor **13**.

Final coupling of the tetrasaccharides (**10** and **13**) to Glc-Cer acceptor **5** led to GM1 ganglioside frameworks **14** and **15**, respectively. Similar to the GM3 analogs, compounds **14** and **15** were subsequently converted into their C9-/C6-amino forms. These underwent further conjugation with the succinimidyl esters of fluorescent dyes to yield the target fluorescent GM1 probes (TMR-S9-GM1, 594-S9-GM1, 488-S9-GM1, and 594-termG6-GM1) [61].

1.1.3. Synthesis of fluorescent GM2 analogs

The S9 GM2 glycan moiety was synthesized using a similar approach to that used for S9 GM1 (Fig. 7). C9-NHTFAc-Neu-Gal acceptor **8** was used to construct the branched trisaccharide. Disaccharide acceptor **8** was glycosylated with *N*-Troc-galactosaminyl donor **17** [71] and then protecting group manipulation resulted in donor **18**. For the GN6 analogs, C6-azido-*N*-trichloroacetyl-galactosaminyl donor **20** was coupled to Neu-Gal acceptor **19** to produce a trisaccharide. Next, the C6-azide group and the C2-trichloroacetyl moiety were converted to either an amine or acetamide group, respectively. These were then treated with TFAcOMe to produce a C6-NHTFAc derivative. Trisaccharide donors (**18** and **21**) were coupled to Glc-Ce acceptor **5** to create the GM2 frameworks **22** and **23**. Finally, the protected GM2-analog precursors were derivatized to produce ATTO594-conjugated GM2 analogs (594-S9-GM2 and 594-GN6-GM2) [61].

1.1.4. Synthesis of the fluorescent GD1b analog

The b-series ganglioside GD1b contains an α(2,8)-linked disialyl moiety

that is particularly difficult to synthetically target due to the low reactivity of 8-OH. Modification of the sialyl donor, such as by substituting 9-OH with an amide group, could greatly decrease stereoselectivity during glycosidation. Therefore, we targeted the C6 position of the terminal Gal as the dye loading position. The glycan part of GD1b could be disassembled into the C6-NHTFAc galactosyl imidate **12**, which is common to termG6 GM1, and disialic acid-containing tetrasaccharide acceptor **24** [56], previously developed by our group (Fig. 8). The coupling of donor **12** and acceptor **24** led to a 70% yield of GD1b core pentasaccharide. This resulting pentasaccharide was sequentially converted into the imidate derivative **25** and coupled with the Glc-Cer cassette to yield fully protected GD1b **26**. Finally, global deprotection and coupling with ATTO594 succinimidyl ester produced 594-termG6-GD1b [61].

1.2. Characterization of the new ganglioside probes

The fluorescent analogs of gangliosides were subjected to biophysical evaluation to examine their raftphilicities. The fluorescent analogs were also compared to native molecules to assess their affinities to bind sugar-binding proteins known to influence dye conjugation and protein recognition. Raft markers, such as cholesterol and saturated phospholipids, were preferentially partitioned into detergent-resistant membranes (DRMs). These are typically insoluble in cold non-ionic detergents. Markers were also partitioned into liquid-ordered phase-like (Lo-like) domains in giant plasma membrane vesicles (GPMVs). These contained the full complement of lipids and proteins found in native PMs, except for the actin-based membrane skeleton [56, 72, 73].

1.2.1. Analysis of DRM partitioning

The cold-detergent solubilities of fluorescent gangliosides synthesized in the study, in addition to commercially available analogs, were examined in human T24 epithelial cells. PMs with pre-incorporated fluorescent ganglioside analogs, and other fluorescent lipids, were treated with cold Triton X-100 and observed by epifluorescence microscopy [74]. This showed that the S9 (GM3, GM2, and GM1), termG6-GM1, GN6-GM2, and termG6-GD1b analogs mainly partitioned into the DRMs (Fig. 9a, c). TMR-G6-GM3 and commercially available BodipyFL-C5-GM1 [75-78], in which a fatty acid chain is substituted with BodipyFL and is widely used as a raft marker, solubilized almost completely in detergent, similar to non-raft markers (BodipyFL-C5-PC, 594-DOPE, and 647N-DOPE) [61]. In the TMR-G6-GM3 derivative, the hydrophobic dye TMR is attached to position C6 of galactose, while in BodipyFL-C5-PC, the hydrophobic dye BodipyFL is attached to the sn-2-acyl chain via a C5 alkyl chain of PC. For both of these markers, the hydrophobic dyes used may hamper their incorporation into DRMs. Analysis of DRM partitioning showed that modification using hydrophilic fluorophores at the S9 position of GM3, including ATTO594, ATTO488, and Fl, retained a preference for the DRM partition.

A discrepancy between the partition patterns of several probes into either the DRM or Lo phase was also observed. For example, TMR-G6-GM3 was almost completely solubilized in cold-Triton X-100 but had an average Lo/Ld ratio of 1.7. This may be due to the fact that these assays were performed in different cell types (T24 cells for DRM and RBL-2H3 cells for Lo/Ld) or because Triton X-100

promotes domain formation [79]. TMR-G6-GM3 may therefore be segregated from these induced domains.

1.2.2. Analysis of Lo-like and Ld-like domain partitioning in GPMVs

Our examination of the partitioning of fluorescent ganglioside analogs into Lo-like and Ld-like domains in GPMVs closely matches previous analyses of partitioning in DRMs (Fig. 9b, c) [61]. These results indicated that only ganglioside analogs modified using hydrophilic fluorophores at the terminal position of the glycan group associated with raft domains, similar to native gangliosides.

1.2.3. Binding affinities of sugar-binding proteins

Surface plasmon resonance (SPR) analysis was used to measure the dissociation constants (K_d) between ganglioside analogs and sugar-binding proteins. The binding affinities of CTB to fluorescent GM1s, and those of WGA to fluorescent GM3s incorporated into 1-palmitoyl-2-oleoyl-sn-glycerophosphorylcholine vesicles (10 mol %), were determined using SPR equilibrium analysis. GM1 and GM3 conjugated with ATTO594 at their S9 positions exhibited comparable affinity constants to native molecules for both of the ganglioside binding proteins, cholera toxin subunit B (CTB) and wheat germ agglutinin (WGA) (Table 1). These results suggest that ATTO594 conjugation at the S9 position of GM1 and GM3 did not interfere with CTB binding to GM1, nor WGA binding to GM3 [61]. In contrast, the affinity of CTB to a previously developed fluorescent GM1 in which Alexa568 has been conjugated to the

glycerol side chain of the sialic acid (with the removal of two hydroxyl groups and one carbon), was reduced by approximately 10-fold [38]. This difference may be due to the location of the dye molecule within the GM1 molecule and/or the particular dye used.

In earlier studies examining the dynamics and functions of gangliosides in PMs, fluorescently labeled CTB (e.g., Cy3-CTB) has widely been used as a GM1-specific marker. However, GM1 molecules labeled using this technique are crosslinked, modifying the distribution of gangliosides and their behavior in PMs. Single-molecule tracking indicated that Cy3-CTB complexed with GM1 moved with smaller diffusion coefficients (0.01–0.06 $\mu m^2/s$) than any of our fluorescent ganglioside analogs (0.31–0.36 $\mu m^2/s$) or phospholipids (0.20–0.22 $\mu m^2/s$). This was due to the clustering of GM1 molecules after binding to five CTB carbohydrate binding pockets. These results clearly show that CTB changes the dynamic behavior of GM1. In this context, previously developed fluorescent GM1 probes, in which a fluorescent dye was directly attached to the lipid via the fatty acid moiety [34-37], have been revealed to be unsuitable markers for lipid rafts.

Our results have also shown that the most widely used marker, BodipyFL-C5-GM1 [75-78], is not incorporated into DRMs nor Lo-like phases, although its diffusion coefficients are similar to that of our fluorescent gangliosides and phospholipids. Dye introduction into the lipid tail moiety may weaken hydrophobic interactions with other molecules residing in the DRMs and Lo-like phase. Recently, a head group-labeled GM1 probe has been developed, in which Alexa568 was conjugated to a shortened side chain of the sialic acid group (one carbon and two hydroxyl groups were removed from the glycerol moiety) [38].

However, it exhibited lower affinity to CTB than native molecules (~10-fold less). This highlights the importance of retaining the glycerol chain of sialic acid when modifying gangliosides. Similarly, another head group-labeled GM1 probe, in which the C5 amino position of sialic acid was conjugated to ATTO647N, showed low-level partitioning to the Lo-like phase in GPMVs [40].

1.3. Behavior of ganglioside analogs in cell PMs

1.3.1. Conjugation of hydrophilic dyes to the terminal residues of gangliosides to create PM raftophilic analogs

As previously described, fluorescently labeled ganglioside-binding proteins have been employed as both GM1 and GM3 markers but these proteins are multivalent and crosslink with gangliosides. This changes the distribution and behavior of gangliosides in the PM. It has consequently been impossible to examine if gangliosides partition into rafts in either steady-state or stimulated cells. We therefore utilized our new fluorescent ganglioside probes to investigate the partitioning of these derivatives in lipid rafts. GPI-anchored proteins are typical markers of raft molecules and congregate in large areas after live cells are incubated with primary and secondary antibodies [80]. We therefore employed the complementary control factor CD59 as a GPI-anchored protein marker of lipid rafts.

Using confocal fluorescence microscopy, we found that our new ganglioside probes partitioned into both the DRM and Lo-like domains, and co-localized with large areas of CD59 staining. It is important to note that such co-localization was observed without any clustering induced by binding proteins,

such as cholera toxin subunit B (CTB) or antibodies. These results indicated that the affinity of GM3 analogs for lipid rafts was highest for 594-S9-GM3, 488-S9-GM3, and Fl-S9-GM3, and then affinities decreased from TMR-S9-GM3 to TMR-G6-GM3. For GM1 analogs, 594-S9-GM1, 594-termG6-GM1, 488-S9-GM1 were all equivalent and had higher affinity than TMR-S9-GM1. However, 647N-S9-GM3, TMR-G6-GM3, and Bodipy-FL-GM1 partitioned into the non-raft fraction and should therefore not be used as markers for lipid rafts. Based on these data, we synthesized and assessed the GM2 and GD1b fluorescent probes, 594-S9-GM2, 594-GN6-GM2, and 594-termG6-GD1b. We found that these probes were concentrated in induced large lipid rafts.

1.3.2. Single-molecule imaging of ganglioside probes, both inside and outside areas stained with CD59

Confocal fluorescence microscopy revealed that the ganglioside probes we have developed co-localized with rafts in PMs, but it is still unclear if these probes dynamically entered and left the raft domains. Single fluorescent-molecule tracking of 594-S9-GM3 and GM1 revealed that both probes diffused in the bulk and regions of CD59 staining (used as a marker of raft regions). Each ganglioside probe was maintained within the boundaries of CD59 patch and the bulk region, rather than passing through. However, the non-raft phospholipid probe 594-DOPE was primarily located outside of the CD59 regions and was repelled at the boundary of the rafts. We found that our ganglioside probes were enriched in the CD59-rich regions by 4- to 10-fold, while 594-DOPE was almost completely excluded. These data are consistent with the confocal fluorescence microscopy

observations and indicate that the large regions containing CD59 form raft domains by transiently recruiting other raft molecules, such as gangliosides.

The 594-S9-GM3 and GM1 molecules found in the large CD59 patches frequently underwent temporal confinement with lifetimes of ~100 ms. We term this process **T**emporal **A**rrest of **L**atera**L** diffusion (TALL). Conversely, almost all of the 594-S9-GM3 and GM1 molecules outside of the CD59 regions were constantly mobile when observed at 33, 8, or 0.5 ms intervals [61]. After actin depolymerization, the fractions of TALL for 594-S9-GM3 and GM1 inside the CD59 regions were significantly decreased, suggesting that antibody-induced CD59 clusters might associate with the actin-based membrane skeleton. Alternatively, they may induce actin polymerization and TALL occurs through indirect (or transbilayer) interactions between gangliosides and actin filaments. This may be due the binding of gangliosides with crosslinked CD59 clusters that are immobilized on actin filaments via an unknown transmembrane protein, or interdigitation of the outer and inner leaflets [81].

A recent study by Sevcsik *et al.* (2015) showed the formation of 3 μm-sized spots of monomeric GFP-GPI (mGFP-GPI) using an anti-GFP antibody coated micropattern did not lead to concentration of CD59, another GPI-anchored protein [82]. The density of mGFP-GPI in the micropattern varied between 500~10,000 molecules/μm^2, and occupied 0.5~11% of the area in the spots. In a study by Komura *et al.* (2016) [61], CD59 was crosslinked by primary and secondary antibodies, producing relatively small clusters less than 3 μm in diameter. These occupied 7.7~20% of the area in the cluster if the average distance between CD59 molecules was 9.6 nm [83] or 6.0 nm [84] and the radius

of CD59 was 1.5 nm [82]. Higher densities of CD59 were able to concentrate the ganglioside probes that Komura *et al.* (2016) developed [61]. This is consistent with the large drop in the diffusion coefficients shown for the probe molecules when the nearest-neighbor distance of steric obstacles was less than 10 nm [82].

1.3.3. Stabilization of GPI-anchored protein cluster rafts through ganglioside recruitment

We next examined raft formation under more physiological conditions. After ligation, CD59 forms stable oligomers that recruit and activate intracellular signaling molecules, including phospholipase Cγ (PLCγ), Src family kinase (SFKs), and trimeric G proteins [85-90]. This eventually leads to intracellular IP_3-Ca^{2+} responses. These CD59 oligomers have been termed "CD59-cluster signaling rafts" and they form under certain physiological conditions. We performed simultaneous two-color single-molecule observations of fluorescent ganglioside probes (GM1 and GM3) and the stable CD59 oligomers that are induced upon ligation.

Both 594-S9-GM1 and GM3 probes were recruited to the stable CD59-cluster signaling rafts where they interacted for an average of approximately 100 ms before separating (Fig. 10a-c). However, the non-raft control phospholipid, 594-DOPE, co-localized with CD59-cluster signaling rafts for much shorter periods of time. After cholesterol depletion, or when using the non-raft chimeric mutant protein CD59-TM, the durations of co-localization were approximately halved. These results indicated that the co-localization of gangliosides and CD59 was not due to an interaction between the headgroup regions of gangliosides and CD59 but was rather due to raft-lipid interactions and the alkyl chains. This is supported

by a recent study examining sphingomyelin and saturated phosphatidylcholine probes [91].

1.3.4. GPI-anchored protein homodimers are stabilized by raft-lipid interactions

In steady state PMs, CD59 forms transient homodimers with a mean lifetime of approximately 160 ms [87, 92]. The lifetime of homodimers was reduced by half after PM cholesterol depletion or after replacing the GPI-anchoring chain of CD59 with a non-raft-associating transmembrane domain. These results suggest that CD59 homodimers are stabilized by raft-lipid interactions.

Single-molecule tracking of 594-S9-GM3 and GM1 showed that gangliosides are transiently recruited to short-lived CD59 homodimers for approximately 80 ms, and to CD59 monomers for 50 ms (Fig. 10c) [61]. The non-raft-associating control 594-DOPE co-localized with CD59 monomers and homodimers for an average of only 40 ms, shorter than the co-localization lifetimes of the gangliosides (Fig. 10c). Transient interactions between gangliosides and both CD59 monomers and homodimers may be due to interactions between glycans and/or the protein moieties of CD59 and glycans and/or lipid moieties. It is interesting that the associating periods of gangliosides and CD59 cluster rafts (approximately 100 ms) were longer than those found for CD59 homodimers (80 ms) and much longer than those shown by CD59 monomers (50 ms). These results support our previous results indicating that CD59 cluster rafts and CD59 homodimers are stabilized by raft-lipid interactions

and raft-lipid interactions may be mediated or strengthened by ganglioside recruitment.

It was previously unknown as to whether clustered raft molecules can recruit other raft components, although when additional raft elements are clustered, both the initial and following raft molecules co-localize with each other [52, 53, 80, 93]. It was also not obvious if these secondary non-crosslinked raft elements can be recruited to clustered raft molecules. Simultaneous single-molecule observations of CD59 and non-crosslinked ganglioside probes have revealed that non-crosslinked gangliosides are transiently recruited to CD59 monomers, CD59 homodimers, CD59-cluster signaling rafts, and CD59 regions. These results are consistent with another study showing that mGFP-GPI dimers induced by a monoclonal antibody transiently recruit other non-crosslinked GPI-anchored proteins [94].

1.3.5. Assessment of the TALL fractions of ganglioside probes by high-speed observations of single-molecule probes

Previous reports have shown that ganglioside probes are temporarily confined in small domains in cell PMs for 10~20 ms. Conversely, control non-raft unsaturated phospholipid probes rarely display TALL [36, 76, 95-97]. In these earlier studies, the fraction of time that gangliosides were confined to the membrane decreased after cholesterol depletion. However, as previously outlined, the ganglioside probes used in this previous work partitioned into non-raft fractions, such as the Ld phase and non-DRMs [40, 61]. We therefore examined whether our new ganglioside probes partitioned into the raft fraction or were

confined to small domains in the PMs of cells. To achieve this, we performed single molecule imaging of 594-S9-GM1, 594-S9-GM3, and 594-DOPE at 0.5 ms intervals at 23°C in PtK2, CHO-K1, T24, and NRK cell types. The TALL of various gangliosides were measured using previously developed methods [96] that were further refined through our studies [87, 98].

Fractions of time in which diffusion was constantly confined to small areas (the immobile fraction) were rarely found for all three tested molecules in each of the cell types. The proportions of time spent in the 100 nm diameter domains were estimated to be 1.7~3.1% for 594-S9-GM3 and GM1 and 4.6~5.2% for 594-DOPE in each of the four cell types. Our new GM1 and GM3 probes were therefore excellent raft markers and spent little time trapped in small membrane domains. This was not the same for the non-raft-associating 594-DOPE control. The results of this investigation into our new ganglioside probes are supported by recent studies reporting new sphingomyelin (SM) and distearoyl phosphatidylcholine (DSPC) probes that partition into the Lo phase and DRM fraction. These probes also did not show any TALL in small domains (100 nm in diameter) when assessed using high-speed observations at 0.5 ms intervals [91]. However, these results are at odds with some previous data [36, 76, 96, 97]. For example, Sahl *et al*. (2010) [96] reported that their SM probe (ATTO647N-SM) had a TALL with a lifetime of 17 ms and the proportion of time the probe spent in small domains was approximately 70% (with an apparent trapped domain 12 nm in diameter) in the basal PMs of PtK2 cells. A phospholipid analog (ATTO647N-DOPE) only exhibited TALL with a lifetime of 3 ms and proportion of time spent in small domains was 30% (with an apparent trapped domain 22 nm in diameter). We

used the same protocol as Sahl *et al*. (2010) to determine TALL using various means, but could only determine a short period of TALL [61, 91].

We also incorporated the lipid probes into cell PMs without bovine serum albumin (BSA) and observed single molecules in cells with low confluency (less than 50%). This was only possible when the fluorophore of the probe is hydrophilic and negatively charged because ganglioside analogs that feature hydrophobic dyes bind strongly to the glass apparatus, whether the probe was adsorbed to BSA or not (unpublished data). Additionally, the confluency of PtK2 cells used by Sahl *et al.* (2010) was relatively high (cells were seeded to a confluency of 80% and lipid probes were observed at 100% cell confluency). As PtK2 cells form tight junctions at high confluencies [99], lipid probes added from cell apical sides accumulate in the apical membrane and are rarely observed in the basal membranes (unpublished data). Due to the fact Sahl *et al.* (2010) observed molecular diffusion at the basal membranes, the lipid composition and membrane structures they observed may be different from those examined in our study. This may be one of the reasons why our results differ from Sahl *et al.* (2010)[96].

A large fraction of ganglioside probes underwent simple Brownian diffusion when observed at 0.5 ms intervals [61]. However, single-molecule imaging of lipids and transmembrane proteins at a higher temporal resolution, such as 25 μs/frame, showed a different type of motion. Briefly, the molecules underwent temporary confinement in a boundary region of the membrane with an average diameter of 30-230 nm. This confinement was interrupted by rare hops (1-50 ms) to adjacent, yet still temporary confining regions, that we have

termed compartments [100-107]. We have named this behavior hop diffusion as the membrane molecules undergo macroscopic diffusion by "hopping" to adjacent compartments, although they freely diffuse within a compartment. In future work to investigate the association between gangliosides, lipid rafts, and membrane structures in more detail, our work suggests that single ganglioside probe molecules should be observed at higher time resolutions.

2. Conclusion

New ganglioside probes that partition into raft domains (DRM, Lo-like domains, and CD59 clusters), and bind to proteins with similar affinity to the parental molecules, can be developed using an entirely chemical-based synthesis method after intensive effort [61]. The conjugation of hydrophilic fluorescent dyes at the appropriate positions within gangliosides (for example, the C9 position of the sialic acid group) is essential for maintaining their properties. Furthermore, as non-specific binding of hydrophilic ganglioside probes to glass is low, they can be easily incorporated into cell PMs without complex formations that incorporate BSA. Single-molecule observations have revealed that the new ganglioside probes we have developed were transiently recruited to CD59 monomers and short-lived homodimers in steady state cells, and also to CD59-cluster signaling rafts and large antibody-induced CD59 patches. This is the first direct observation of an association between gangliosides and a GPI-anchored protein without involving crosslinking of gangliosides nor artifacts. This demonstrates that gangliosides and GPI-anchored proteins dynamically associate with each other in a cholesterol-dependent manner within milliseconds. These

results also indicated that CD59 cluster rafts and CD59 homodimers are stabilized by raft-lipid interactions that may be mediated or strengthened by ganglioside recruitment. Such a finding would not have been possible without naturally behaving fluorescent ganglioside analogs and single-molecule imaging. When gangliosides are crosslinked by proteins such as CTB and WGA, their diffusion slows, or even stops, and it appears that gangliosides interact with GPI-anchored protein clusters for very long periods of time [61].

Gangliosides play important roles in a wide variety of physiological functions, including the regulation of receptor activity. However, the specific mechanisms that underlie these roles are unclear because gangliosides have never directly been observed in living cell PMs due to a lack of functional analogs. The new fluorescent ganglioside probes we have developed behave similarly to parental molecules and will facilitate studies to elucidate these mechanisms.

Acknowledgements

This work was supported in part by Grants-in-Aids for Innovative Areas grants to K.G.M.S. [2311001 and 16H01358] and H. A. [24110505 and 26110704], various Scientific Research grants from the Japan Society for the Promotion of Science (Kiban B awarded to K.G.N.S. [24370055 and 15H04351], H.A. [15H04495], M.K. [22380067], Wakate A awarded to H. A. [23688014], and Kiban S awarded to A.K. [16H06386]), a grant from the Core Research for Evolutional Science and technology (CREST) project "Creation of Fundamental Technologies for Understanding and Control of Biosystem Dynamics" funded by the Japan Science and Technology Agency (JST) awarded to A. K., a grant from the Naito foundation

and Daiichi-Sankyo foundation awarded to K. G. N. S, and by a grant from the Mizutani Foundation awarded to K. G. N. S. and H. A. WPI-iCeMS of Kyoto University is supported by the World Premiere Research Center Initiative (WPI) of MEXT.

References

[1] K. Furukawa, Y. Ohmi, Y. Ohkawa, O. Tajima, K. Furukawa, Glycosphingolipids in the regulation of the nervous system, Advances in neurobiology, 9 (2014) 307-320.

[2] R.L. Schnaar, Gangliosides of the Vertebrate Nervous System, Journal of molecular biology, 428 (2016) 3325-3336.

[3] D.C. Smith, J.M. Lord, L.M. Roberts, L. Johannes, Glycosphingolipids as toxin receptors, Semin Cell Dev Biol, 15 (2004) 397-408.

[4] F.E. Fleming, R. Bohm, V.T. Dang, G. Holloway, T. Haselhorst, P.D. Madge, J. Deveryshetty, X. Yu, H. Blanchard, M. von Itzstein, B.S. Coulson, Relative roles of GM1 ganglioside, N-acylneuraminic acids, and alpha2beta1 integrin in mediating rotavirus infection, J Virol, 88 (2014) 4558-4571.

[5] B.S. Blaum, M. Frank, R.C. Walker, U. Neu, T. Stehle, Complement Factor H and Simian Virus 40 bind the GM1 ganglioside in distinct conformations, Glycobiology, 26 (2016) 532-539.

[6] A.J. Yates, A. Rampersaud, Sphingolipids as receptor modulators. An overview, Annals of the New York Academy of Sciences, 845 (1998) 57-71.

[7] E.G. Bremer, S. Hakomori, D.F. Bowen-Pope, E. Raines, R. Ross, Ganglioside-mediated modulation of cell growth, growth factor binding, and receptor phosphorylation, The Journal of biological chemistry, 259 (1984) 6818-6825.

[8] E.G. Bremer, J. Schlessinger, S. Hakomori, Ganglioside-mediated modulation of cell growth. Specific effects of GM3 on tyrosine phosphorylation of the epidermal growth factor receptor, The Journal of biological chemistry, 261 (1986) 2434-2440.

[9] S.J. Yoon, K. Nakayama, T. Hikita, K. Handa, S.I. Hakomori, Epidermal growth factor receptor tyrosine kinase is modulated by GM3 interaction with N-linked GlcNAc termini of the receptor, Proc Natl Acad Sci U S A, 103 (2006) 18987-18991.

[10] N. Kawashima, S.J. Yoon, K. Itoh, K. Nakayama, Tyrosine kinase activity of epidermal growth factor receptor is regulated by GM3 binding through carbohydrate to carbohydrate interactions, The Journal of biological chemistry, 284 (2009) 6147-6155.

[11] U. Coskun, M. Grzybek, D. Drechsel, K. Simons, Regulation of human EGF receptor by

lipids, Proc Natl Acad Sci U S A, 108 (2011) 9044-9048.
[12] Y. Fukuda, T. Fukui, C. Hikichi, T. Ishikawa, K. Murate, T. Adachi, H. Imai, K. Fukuhara, A. Ueda, A.P. Kaplan, T. Mutoh, Neurotropin promotes NGF signaling through interaction of GM1 ganglioside with Trk neurotrophin receptor in PC12 cells, Brain Res, 1596 (2015) 13-21.
[13] M. Aureli, L. Mauri, M.G. Ciampa, A. Prinetti, G. Toffano, C. Secchieri, S. Sonnino, GM1 Ganglioside: Past Studies and Future Potential, Mol Neurobiol, 53 (2016) 1824-1842.
[14] Y. Ohkawa, S. Miyazaki, K. Hamamura, M. Kambe, M. Miyata, O. Tajima, Y. Ohmi, Y. Yamauchi, K. Furukawa, K. Furukawa, Ganglioside GD3 enhances adhesion signals and augments malignant properties of melanoma cells by recruiting integrins to glycolipid-enriched microdomains, The Journal of biological chemistry, 285 (2010) 27213-27223.
[15] W.R. Jung, H.G. Kim, M.K. Shin, D.I. Park, K.L. Kim, The effect of ganglioside GQ1b on the NMDA receptor signaling pathway in H19-7 cells and rat hippocampus, Neuroscience, 165 (2010) 159-167.
[16] N. Yuki, T. Taki, F. Inagaki, T. Kasama, M. Takahashi, K. Saito, S. Handa, T. Miyatake, A bacterium lipopolysaccharide that elicits Guillain-Barre syndrome has a GM1 ganglioside-like structure, The Journal of experimental medicine, 178 (1993) 1771-1775.
[17] M. Kuwahara, S. Suzuki, K. Takada, S. Kusunoki, Antibodies to LM1 and LM1-containing ganglioside complexes in Guillain-Barre syndrome and chronic inflammatory demyelinating polyneuropathy, Journal of neuroimmunology, 239 (2011) 87-90.
[18] S. Kusunoki, K. Kaida, Antibodies against ganglioside complexes in Guillain-Barre syndrome and related disorders, Journal of neurochemistry, 116 (2011) 828-832.
[19] L. Mauri, R. Casellato, M.G. Ciampa, Y. Uekusa, K. Kato, K. Kaida, M. Motoyama, S. Kusunoki, S. Sonnino, Anti-GM1/GD1a complex antibodies in GBS sera specifically recognize the hybrid dimer GM1-GD1a, Glycobiology, 22 (2012) 352-360.
[20] R. Takahashi, N. Yuki, Streptococcal IdeS: therapeutic potential for Guillain-Barre syndrome, Scientific reports, 5 (2015) 10809.
[21] M. Morikawa, M. Kuwahara, R. Ueno, M. Samukawa, Y. Hamada, S. Kusunoki, Serological study using glycoarray for detecting antibodies to glycolipids and glycolipid complexes in immune-mediated neuropathies, Journal of neuroimmunology, 301 (2016) 35-40.
[22] K. Yanagisawa, A. Odaka, N. Suzuki, Y. Ihara, GM1 ganglioside-bound amyloid beta-protein (A beta): a possible form of preamyloid in Alzheimer's disease, Nature medicine, 1 (1995) 1062-1066.
[23] K. Matsuzaki, How do membranes initiate Alzheimer's Disease? Formation of toxic amyloid fibrils by the amyloid beta-protein on ganglioside clusters, Accounts of chemical research, 47 (2014) 2397-2404.

[24] H. Ueno, T. Yamaguchi, S. Fukunaga, Y. Okada, Y. Yano, M. Hoshino, K. Matsuzaki, Comparison between the aggregation of human and rodent amyloid beta-proteins in GM1 ganglioside clusters, Biochemistry, 53 (2014) 7523-7530.
[25] K. Yanagisawa, GM1 ganglioside and Alzheimer's disease, Glycoconj J, 32 (2015) 87-91.
[26] S. Okada, J.S. O'Brien, Generalized gangliosidosis: beta-galactosidase deficiency, Science, 160 (1968) 1002-1004.
[27] J. Matsuda, O. Suzuki, A. Oshima, Y. Yamamoto, A. Noguchi, K. Takimoto, M. Itoh, Y. Matsuzaki, Y. Yasuda, S. Ogawa, Y. Sakata, E. Nanba, K. Higaki, Y. Ogawa, L. Tominaga, K. Ohno, H. Iwasaki, H. Watanabe, R.O. Brady, Y. Suzuki, Chemical chaperone therapy for brain pathology in G(M1)-gangliosidosis, Proc Natl Acad Sci U S A, 100 (2003) 15912-15917.
[28] M. Jeyakumar, R. Thomas, E. Elliot-Smith, D.A. Smith, A.C. van der Spoel, A. d'Azzo, V.H. Perry, T.D. Butters, R.A. Dwek, F.M. Platt, Central nervous system inflammation is a hallmark of pathogenesis in mouse models of GM1 and GM2 gangliosidosis, Brain : a journal of neurology, 126 (2003) 974-987.
[29] A. Tessitore, P.M.M. del, R. Sano, Y. Ma, L. Mann, A. Ingrassia, E.D. Laywell, D.A. Steindler, L.M. Hendershot, A. d'Azzo, GM1-ganglioside-mediated activation of the unfolded protein response causes neuronal death in a neurodegenerative gangliosidosis, Molecular cell, 15 (2004) 753-766.
[30] A. Fujita, J. Cheng, M. Hirakawa, K. Furukawa, S. Kusunoki, T. Fujimoto, Gangliosides GM1 and GM3 in the living cell membrane form clusters susceptible to cholesterol depletion and chilling, Mol Biol Cell, 18 (2007) 2112-2122.
[31] D. Lingwood, B. Binnington, T. Rog, I. Vattulainen, M. Grzybek, U. Coskun, C.A. Lingwood, K. Simons, Cholesterol modulates glycolipid conformation and receptor activity, Nat Chem Biol, 7 (2011) 260-262.
[32] B.P. Head, H.H. Patel, P.A. Insel, Interaction of membrane/lipid rafts with the cytoskeleton: impact on signaling and function: membrane/lipid rafts, mediators of cytoskeletal arrangement and cell signaling, Biochim Biophys Acta, 1838 (2014) 532-545.
[33] T.R. Galimzyanov, A.S. Lyushnyak, V.V. Aleksandrova, L.A. Shilova, Mikhalyov, II, I.M. Molotkovskaya, S.A. Akimov, O.V. Batishchev, Line Activity of Ganglioside GM1 Regulates the Raft Size Distribution in a Cholesterol-Dependent Manner, Langmuir, 33 (2017) 3517-3524.
[34] G. Schwarzmann, M. Wendeler, K. Sandhoff, Synthesis of novel NBD-GM1 and NBD-GM2 for the transfer activity of GM2-activator protein by a FRET-based assay system, Glycobiology, 15 (2005) 1302-1311.
[35] D. Marushchak, N. Gretskaya, I. Mikhalyov, L.B. Johansson, Self-aggregation--an intrinsic property of G(M1) in lipid bilayers, Mol Membr Biol, 24 (2007) 102-112.

[36] C. Eggeling, C. Ringemann, R. Medda, G. Schwarzmann, K. Sandhoff, S. Polyakova, V.N. Belov, B. Hein, C. von Middendorff, A. Schonle, S.W. Hell, Direct observation of the nanoscale dynamics of membrane lipids in a living cell, Nature, 457 (2009) 1159-1162.
[37] S.M. Polyakova, V.N. Belov, S.F. Yan, C. Eggeling, C. Ringemann, G. Schwarzmann, A. de Meijere, S.W. Hell, New GM1 Ganglioside Derivatives for Selective Single and Double Labelling of the Natural Glycosphingolipid Skeleton, European Journal of Organic Chemistry, 2009 (2009) 5162-5177.
[38] D.J. Chinnapen, W.T. Hsieh, Y.M. te Welscher, D.E. Saslowsky, L. Kaoutzani, E. Brandsma, L. D'Auria, H. Park, J.S. Wagner, K.R. Drake, M. Kang, T. Benjamin, M.D. Ullman, C.E. Costello, A.K. Kenworthy, T. Baumgart, R.H. Massol, W.I. Lencer, Lipid sorting by ceramide structure from plasma membrane to ER for the cholera toxin receptor ganglioside GM1, Dev Cell, 23 (2012) 573-586.
[39] F. Schneider, D. Waithe, M.P. Clausen, S. Galiani, T. Koller, G. Ozhan, C. Eggeling, E. Sezgin, Diffusion of lipids and GPI-anchored proteins in actin-free plasma membrane vesicles measured by STED-FCS, Mol Biol Cell, (2017).
[40] E. Sezgin, I. Levental, M. Grzybek, G. Schwarzmann, V. Mueller, A. Honigmann, V.N. Belov, C. Eggeling, U. Coskun, K. Simons, P. Schwille, Partitioning, diffusion, and ligand binding of raft lipid analogs in model and cellular plasma membranes, Biochim Biophys Acta, 1818 (2012) 1777-1784.
[41] B.J. Nichols, GM1-containing lipid rafts are depleted within clathrin-coated pits, Current biology : CB, 13 (2003) 686-690.
[42] O.O. Glebov, B.J. Nichols, Lipid raft proteins have a random distribution during localized activation of the T-cell receptor, Nature cell biology, 6 (2004) 238-243.
[43] J. Buschiazzo, C. Ialy-Radio, J. Auer, J.P. Wolf, C. Serres, B. Lefevre, A. Ziyyat, Cholesterol depletion disorganizes oocyte membrane rafts altering mouse fertilization, PLoS One, 8 (2013) e62919.
[44] M. Calamai, F.S. Pavone, Partitioning and confinement of GM1 ganglioside induced by amyloid aggregates, FEBS Lett, 587 (2013) 1385-1391.
[45] M.P. Clausen, E.C. Arnspang, B. Ballou, J.E. Bear, B.C. Lagerholm, Simultaneous multi-species tracking in live cells with quantum dot conjugates, PLoS One, 9 (2014) e97671.
[46] K.M. Spillane, J. Ortega-Arroyo, G. de Wit, C. Eggeling, H. Ewers, M.I. Wallace, P. Kukura, High-speed single-particle tracking of GM1 in model membranes reveals anomalous diffusion due to interleaflet coupling and molecular pinning, Nano Lett, 14 (2014) 5390-5397.
[47] M. Calamai, E. Evangelisti, R. Cascella, N. Parenti, C. Cecchi, M. Stefani, F. Pavone, Single molecule experiments emphasize GM1 as a key player of the different cytotoxicity of structurally distinct Abeta1-42 oligomers, Biochim Biophys Acta, 1858 (2016) 386-392.

[48] A.T. Hammond, F.A. Heberle, T. Baumgart, D. Holowka, B. Baird, G.W. Feigenson, Crosslinking a lipid raft component triggers liquid ordered-liquid disordered phase separation in model plasma membranes, Proc Natl Acad Sci U S A, 102 (2005) 6320-6325.
[49] D. Lingwood, J. Ries, P. Schwille, K. Simons, Plasma membranes are poised for activation of raft phase coalescence at physiological temperature, Proc Natl Acad Sci U S A, 105 (2008) 10005-10010.
[50] H.J. Kaiser, D. Lingwood, I. Levental, J.L. Sampaio, L. Kalvodova, L. Rajendran, K. Simons, Order of lipid phases in model and plasma membranes, Proc Natl Acad Sci U S A, 106 (2009) 16645-16650.
[51] M. Stefl, R. Sachl, J. Humpolickova, M. Cebecauer, R. Machan, M. Kolarova, L.B. Johansson, M. Hof, Dynamics and size of cross-linking-induced lipid nanodomains in model membranes, Biophys J, 102 (2012) 2104-2113.
[52] A. Kusumi, K. Suzuki, Toward understanding the dynamics of membrane-raft-based molecular interactions, Biochim Biophys Acta, 1746 (2005) 234-251.
[53] K.A. Tanaka, K.G. Suzuki, Y.M. Shirai, S.T. Shibutani, M.S. Miyahara, H. Tsuboi, M. Yahara, A. Yoshimura, S. Mayor, T.K. Fujiwara, A. Kusumi, Membrane molecules mobile even after chemical fixation, Nat Methods, 7 (2010) 865-866.
[54] H. Ando, Y. Koike, H. Ishida, M. Kiso, Extending the possibility of an N-Troc-protected sialic acid donor toward variant sialo-glycoside synthesis, Tetrahedron Letters, 44 (2003) 6883-6886.
[55] H. Ando, Y. Koike, S. Koizumi, H. Ishida, M. Kiso, 1,5-Lactamized sialyl acceptors for various disialoside syntheses: novel method for the synthesis of glycan portions of Hp-s6 and HLG-2 gangliosides, Angew Chem Int Ed Engl, 44 (2005) 6759-6763.
[56] A. Imamura, H. Ando, H. Ishida, M. Kiso, Ganglioside GQ1b: efficient total synthesis and the expansion to synthetic derivatives to elucidate its biological roles, The Journal of organic chemistry, 74 (2009) 3009-3023.
[57] Y. Iwayama, H. Ando, H. Ishida, M. Kiso, A first total synthesis of ganglioside HLG-2, Chemistry, 15 (2009) 4637-4648.
[58] H. Tamai, H. Ando, H.N. Tanaka, R. Hosoda-Yabe, T. Yabe, H. Ishida, M. Kiso, The total synthesis of the neurogenic ganglioside LLG-3 isolated from the starfish Linckia laevigata, Angew Chem Int Ed Engl, 50 (2011) 2330-2333.
[59] K. Fujikawa, The first total synthesis of ganglioside GalNAc-GD1a, a target molecule for autoantibodies in Guillain-Barre Syndrome, Chemistry A European Journal, 17 (2011) 5641-5651.
[60] S. Nakashima, H. Ando, R. Saito, H. Tamai, H. Ishida, M. Kiso, Efficiently synthesizing lacto-ganglio-series gangliosides by using a glucosyl ceramide cassette approach: the total

synthesis of ganglioside X2, Chemistry, an Asian journal, 7 (2012) 1041-1051.
[61] N. Komura, K.G. Suzuki, H. Ando, M. Konishi, M. Koikeda, A. Imamura, R. Chadda, T.K. Fujiwara, H. Tsuboi, R. Sheng, W. Cho, K. Furukawa, K. Furukawa, Y. Yamauchi, H. Ishida, A. Kusumi, M. Kiso, Raft-based interactions of gangliosides with a GPI-anchored receptor, Nat Chem Biol, 12 (2016) 402-410.
[62] S. Neuenhofer, G. Schwarzmann, H. Egge, K. Sandhoff, Synthesis of lysogangliosides, Biochemistry, 24 (1985) 525-532.
[63] D. Acquotti, S. Sonnino, M. Masserini, L. Casella, G. Fronza, G. Tettamanti, A new chemical procedure for the preparation of gangliosides carrying fluorescent or paramagnetic probes on the lipid moiety, Chemistry and physics of lipids, 40 (1986) 71-86.
[64] M. Wilchek, S. Spiegel, Y. Spiegel, Fluorescent reagents for the labeling of glycoconjugates in solution and on cell surfaces, Biochemical and biophysical research communications, 92 (1980) 1215-1222.
[65] J.R. Rich, A.M. Cunningham, M. Gilbert, S.G. Withers, Glycosphingolipid synthesis employing a combination of recombinant glycosyltransferases and an endoglycoceramidase glycosynthase, Chemical communications (Cambridge, England), 47 (2011) 10806-10808.
[66] G.Y. Yang, C. Li, M. Fischer, C.W. Cairo, Y. Feng, S.G. Withers, A FRET probe for cell-based imaging of ganglioside-processing enzyme activity and high-throughput screening, Angew Chem Int Ed Engl, 54 (2015) 5389-5393.
[67] K. Simons, W.L. Vaz, Model systems, lipid rafts, and cell membranes, Annual review of biophysics and biomolecular structure, 33 (2004) 269-295.
[68] P.S. Niemela, M.T. Hyvonen, I. Vattulainen, Influence of chain length and unsaturation on sphingomyelin bilayers, Biophys J, 90 (2006) 851-863.
[69] T. Fuse, H. Ando, A. Imamura, N. Sawada, H. Ishida, M. Kiso, T. Ando, S.C. Li, Y.T. Li, Synthesis and enzymatic susceptibility of a series of novel GM2 analogs, Glycoconj J, 23 (2006) 329-343.
[70] T. Yoshikawa, Y. Kato, N. Yuki, T. Yabe, H. Ishida, M. Kiso, A highly efficient construction of GM1 epitope tetrasaccharide and its conjugation with KLH, Glycoconj J, 25 (2008) 545-553.
[71] A. Imamura, H. Ando, H. Ishida, M. Kiso, Di-tert-butylsilylene-directed alpha-selective synthesis of 4-methylumbelliferyl T-antigen, Organic letters, 7 (2005) 4415-4418.
[72] T. Baumgart, A.T. Hammond, P. Sengupta, S.T. Hess, D.A. Holowka, B.A. Baird, W.W. Webb, Large-scale fluid/fluid phase separation of proteins and lipids in giant plasma membrane vesicles, Proc Natl Acad Sci U S A, 104 (2007) 3165-3170.
[73] I. Levental, M. Grzybek, K. Simons, Raft domains of variable properties and compositions in plasma membrane vesicles, Proc Natl Acad Sci U S A, 108 (2011) 11411-11416.

[74] A.K. Kenworthy, B.J. Nichols, C.L. Remmert, G.M. Hendrix, M. Kumar, J. Zimmerberg, J. Lippincott-Schwartz, Dynamics of putative raft-associated proteins at the cell surface, J Cell Biol, 165 (2004) 735-746.
[75] D.R. Taylor, N.T. Watt, W.S. Perera, N.M. Hooper, Assigning functions to distinct regions of the N-terminus of the prion protein that are involved in its copper-stimulated, clathrin-dependent endocytosis, Journal of cell science, 118 (2005) 5141-5153.
[76] P.F. Lenne, Dynamic molecular confinement in the plasma membrane by microdomains and the cytoskeleton meshwork, EMBO J., 25 (2006) 3245-3256.
[77] R. Jones, E. Howes, P.D. Dunne, P. James, A. Bruckbauer, D. Klenerman, Tracking diffusion of GM1 gangliosides and zona pellucida binding molecules in sperm plasma membranes following cholesterol efflux, Dev Biol, 339 (2010) 398-406.
[78] D. Svistounov, A. Warren, G.P. McNerney, D.M. Owen, D. Zencak, S.N. Zykova, H. Crane, T. Huser, R.J. Quinn, B. Smedsrod, D.G. Le Couteur, V.C. Cogger, The Relationship between fenestrations, sieve plates and rafts in liver sinusoidal endothelial cells, PLoS One, 7 (2012) e46134.
[79] H. Heerklotz, Triton promotes domain formation in lipid raft mixtures, Biophys J, 83 (2002) 2693-2701.
[80] T. Harder, Scheiffele, P., Verkade, P., Simons, K., Lipid domain structure of the plasma membrane revealed by patching of membrane compartments, J. Cell Biol., 141 (1998) 929-942.
[81] R. Raghupathy, A.A. Anilkumar, A. Polley, P.P. Singh, M. Yadav, C. Johnson, S. Suryawanshi, V. Saikam, S.D. Sawant, A. Panda, Z. Guo, R.A. Vishwakarma, M. Rao, S. Mayor, Transbilayer lipid interactions mediate nanoclustering of lipid-anchored proteins, Cell, 161 (2015) 581-594.
[82] E. Sevcsik, M. Brameshuber, M. Folser, J. Weghuber, A. Honigmann, G.J. Schutz, GPI-anchored proteins do not reside in ordered domains in the live cell plasma membrane, Nat Commun, 6 (2015) 6969.
[83] T.C. Werner, J.R. Bunting, R.E. Cathou, The shape of immunoglobulin G molecules in solution, Proc Natl Acad Sci U S A, 69 (1972) 795-799.
[84] E.A. Hewat, D. Blaas, Structure of a neutralizing antibody bound bivalently to human rhinovirus 2, The EMBO journal, 15 (1996) 1515-1523.
[85] K.G. Suzuki, T.K. Fujiwara, F. Sanematsu, R. Iino, M. Edidin, A. Kusumi, GPI-anchored receptor clusters transiently recruit Lyn and G alpha for temporary cluster immobilization and Lyn activation: single-molecule tracking study 1, J Cell Biol, 177 (2007) 717-730.
[86] K.G. Suzuki, T.K. Fujiwara, M. Edidin, A. Kusumi, Dynamic recruitment of phospholipase C gamma at transiently immobilized GPI-anchored receptor clusters induces

IP3-Ca2+ signaling: single-molecule tracking study 2, J Cell Biol, 177 (2007) 731-742.
[87] K.G. Suzuki, R.S. Kasai, K.M. Hirosawa, Y.L. Nemoto, M. Ishibashi, Y. Miwa, T.K. Fujiwara, A. Kusumi, Transient GPI-anchored protein homodimers are units for raft organization and function, Nat Chem Biol, 8 (2012) 774-783.
[88] K.G. Suzuki, Lipid rafts generate digital-like signal transduction in cell plasma membranes, Biotechnol J, 7 (2012) 753-761.
[89] K.G. Suzuki, New insights into the organization of plasma membrane and its role in signal transduction, Int Rev Cell Mol Biol, 317 (2015) 67-96.
[90] K.G. Suzuki, Single-Molecule Imaging of Signal Transduction via GPI-Anchored Receptors, Methods in molecular biology (Clifton, N.J.), 1376 (2016) 229-238.
[91] M. Kinoshita, K.G. Suzuki, N. Matsumori, M. Takada, H. Ano, K. Morigaki, M. Abe, A. Makino, T. Kobayashi, K.M. Hirosawa, T.K. Fujiwara, A. Kusumi, M. Murata, Raft-based sphingomyelin interactions revealed by new fluorescent sphingomyelin analogs, J Cell Biol, 216 (2017) 1183-1204.
[92] K.G. Suzuki, R.S. Kasai, T.K. Fujiwara, A. Kusumi, Single-molecule imaging of receptor-receptor interactions, Methods in cell biology, 117 (2013) 373-390.
[93] S.R. Mayor, K. G. Maxfield, F. R., Sequestration of GPI-anchored proteins in caveolae traggered by cross-linking, Science, 264 (1994) 1948-1951.
[94] H. Huang, M.F. Simsek, W. Jin, A. Pralle, Effect of receptor dimerization on membrane lipid raft structure continuously quantified on single cells by camera based fluorescence correlation spectroscopy, PLoS One, 10 (2015) e0121777.
[95] A. Honigmann, V. Mueller, H. Ta, A. Schoenle, E. Sezgin, S.W. Hell, C. Eggeling, Scanning STED-FCS reveals spatiotemporal heterogeneity of lipid interaction in the plasma membrane of living cells, Nat Commun, 5 (2014) 5412.
[96] S.J. Sahl, M. Leutenegger, M. Hilbert, S.W. Hell, C. Eggeling, Fast molecular tracking maps nanoscale dynamics of plasma membrane lipids, Proc Natl Acad Sci U S A, 107 (2010) 6829-6834.
[97] J. Wenger, F. Conchonaud, J. Dintinger, L. Wawrezinieck, T.W. Ebbesen, H. Rigneault, D. Marguet, P.F. Lenne, Diffusion analysis within single nanometric apertures reveals the ultrafine cell membrane organization, Biophys J, 92 (2007) 913-919.
[98] A.C. Shibata, T.K. Fujiwara, L. Chen, K.G. Suzuki, Y. Ishikawa, Y.L. Nemoto, Y. Miwa, Z. Kalay, R. Chadda, K. Naruse, A. Kusumi, Archipelago architecture of the focal adhesion: membrane molecules freely enter and exit from the focal adhesion zone, Cytoskeleton (Hoboken, N.J.), 69 (2012) 380-392.
[99] Y. Ando-Akatsuka, M. Saitou, T. Hirase, M. Kishi, A. Sakakibara, M. Itoh, S. Yonemura, M. Furuse, S. Tsukita, Interspecies diversity of the occludin sequence: cDNA cloning of

human, mouse, dog, and rat-kangaroo homologues, J Cell Biol, 133 (1996) 43-47.
[100] T. Fujiwara, K. Ritchie, H. Murakoshi, K. Jacobson, A. Kusumi, Phospholipids undergo hop diffusion in compartmentalized cell membrane, J Cell Biol, 157 (2002) 1071-1081.
[101] A. Kusumi, C. Nakada, K. Ritchie, K. Murase, K. Suzuki, H. Murakoshi, R.S. Kasai, J. Kondo, T. Fujiwara, Paradigm shift of the plasma membrane concept from the two-dimensional continuum fluid to the partitioned fluid: high-speed single-molecule tracking of membrane molecules, Annual review of biophysics and biomolecular structure, 34 (2005) 351-378.
[102] K. Suzuki, K. Ritchie, E. Kajikawa, T. Fujiwara, A. Kusumi, Rapid hop diffusion of a G-protein-coupled receptor in the plasma membrane as revealed by single-molecule techniques, Biophys J, 88 (2005) 3659-3680.
[103] A. Kusumi, Y.M. Shirai, I. Koyama-Honda, K.G. Suzuki, T.K. Fujiwara, Hierarchical organization of the plasma membrane: investigations by single-molecule tracking vs. fluorescence correlation spectroscopy, FEBS Lett, 584 (2010) 1814-1823.
[104] A. Kusumi, K.G. Suzuki, R.S. Kasai, K. Ritchie, T.K. Fujiwara, Hierarchical mesoscale domain organization of the plasma membrane, Trends in biochemical sciences, 36 (2011) 604-615.
[105] A. Kusumi, T.K. Fujiwara, R. Chadda, M. Xie, T.A. Tsunoyama, Z. Kalay, R.S. Kasai, K.G. Suzuki, Dynamic organizing principles of the plasma membrane that regulate signal transduction: commemorating the fortieth anniversary of Singer and Nicolson's fluid-mosaic model, Annual review of cell and developmental biology, 28 (2012) 215-250.
[106] A. Kusumi, T.K. Fujiwara, N. Morone, K.J. Yoshida, R. Chadda, M. Xie, R.S. Kasai, K.G. Suzuki, Membrane mechanisms for signal transduction: the coupling of the meso-scale raft domains to membrane-skeleton-induced compartments and dynamic protein complexes, Semin Cell Dev Biol, 23 (2012) 126-144.
[107] T.K. Fujiwara, K. Iwasawa, Z. Kalay, T.A. Tsunoyama, Y. Watanabe, Y.M. Umemura, H. Murakoshi, K.G. Suzuki, Y.L. Nemoto, N. Morone, A. Kusumi, Confined diffusion of transmembrane proteins and lipids induced by the same actin meshwork lining the plasma membrane, Mol Biol Cell, 27 (2016) 1101-1119.

Figure Legends

Fig. 1. An overview of the variety of roles that gangliosides play in the physiological functions of cell membranes. For example, gangliosides are involved in the regulation of membrane receptor activity (Left), the formation of raft domains, of which they are one of the most important components (Middle), and the invasion of bacteria, microbial toxins, and viruses into cells (Right).

Fig. 2. Fluorescent analogs of GM1 derived from natural GM1.

Fig. 3. A fluorescent analog of GM3 synthesized using a chemoenzymatic method.

Fig. 4. Fluorescent analogs of gangliosides synthesized using a chemical method.

Fig. 5. Outline of the synthetic routes used to create fluorescent analogs of GM3. MP = *p*-methoxybenzyl; Bn = benzyl; Troc = 2,2,2-trichloroethoxycarbonyl; Bz = benzoyl; TFAc = trifluoroacetyl; PMB = *p*-methoxybenzyl.

Fig. 6. Outline of the synthetic routes used to create fluorescent analogs of GM1.

Fig. 7. Outline of the synthetic routes used to create fluorescent analogs of GM2. TCA = trichloroacetyl.

Fig. 8. Outline of the synthetic routes used to create fluorescent analogs of GD1b. SE = 2-(trimethylsilyl)ethyl.

Fig. 9. Partitioning of fluorescent ganglioside analogs. (A) Fluorescence images of 594-S9-GM3, before and after treatment of T24 cells with cold-Triton X-100. (B) Fluorescence images of 594-S9-GM1 and BodipyFL-PC, showing how they are partitioned into Lo- and Ld-like domains in GPMVs. (C) The second column contains the ratios of the fluorescence intensities for probes that remained in cell PMs after cold-Triton X-100 relative to intact cell PMs. The third column contains the ratios of probes in the Lo phase of GPMVs relative to the Ld phase.

Fig. 10. Single-molecule observations of ganglioside probes and CD59. Ganglioside probes were frequently and transiently recruited to CD59 homodimer rafts and CD59-cluster signaling rafts [43]. (A) Typical video-frame sequences of simultaneous observations of single 594-S9-GM3 molecules and CD59-cluster signaling rafts. The co-localization period was between frames 6 and 9. A time course is shown above the images. (B) The trajectories of single 594-S9-GM3 molecules and CD59-cluster rafts shown in (A). Co-localization within 240 nm is shown in the blue (594-S9-GM3) and orange (CD59-cluster raft) trajectories.
(C) A schematic of the transient recruitment of gangliosides (GM1 and GM3) to CD59 monomers, transient homodimer rafts (with a lifetime of 160 ms), and CD59-cluster signaling rafts continuing for 12, 40, and 48 ms. The transient interactions between gangliosides and each of these forms of CD59 in the PMs was dependent on raft-lipid interactions. Transient CD59 monomers and homodimers converted between each other frequently in steady-state cells. However, after stimulation, CD59-cluster signaling rafts formed that were highly

stable and lasted for several minutes.

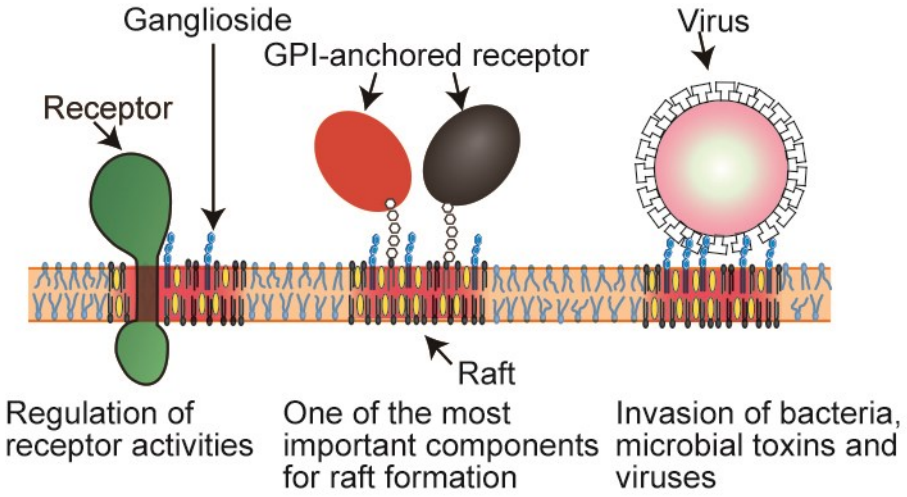

Figure 1. An overview of the variety of roles that gangliosides play in the physiological functions of cell membranes.

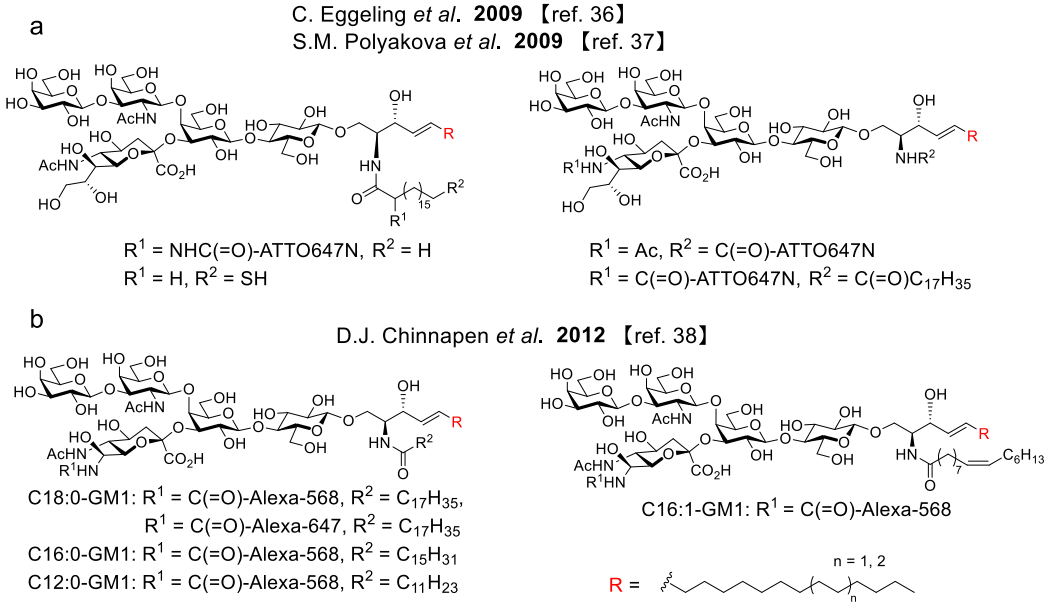

Figure. 2 Fluorescent analogs of GM1 derived from natural GM1

G.Y. Yang *et al*. **2015** 【ref. 66】

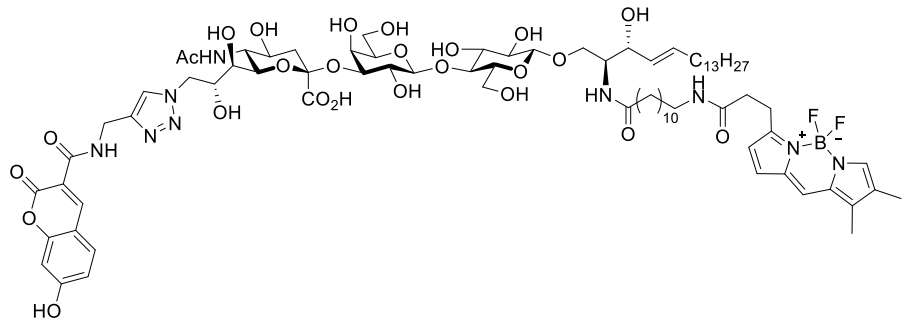

Figure 3. Fluorescent analog of GM3 synthesized by a chemoenzymatic method

N. Komura *et al*. **2016** 【ref. 61】

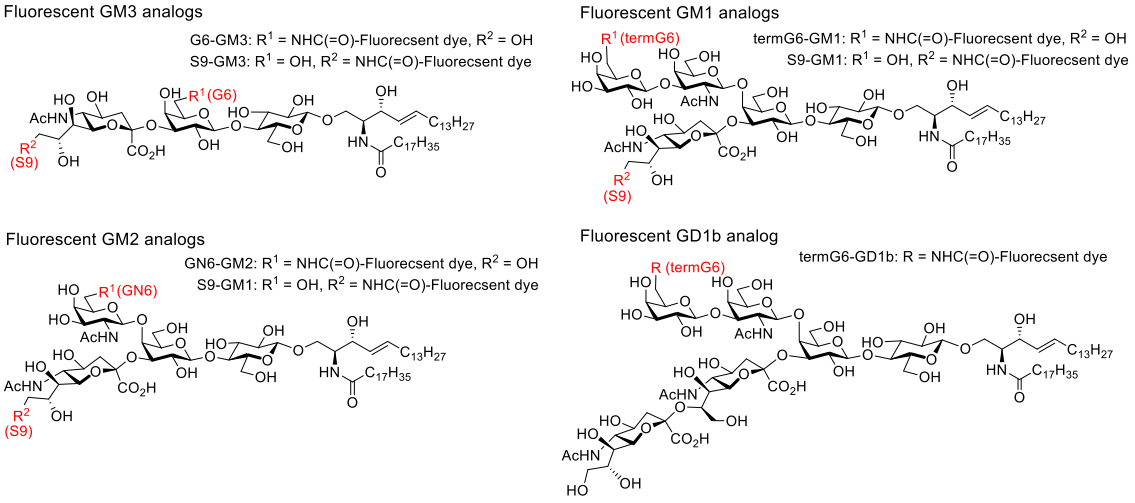

Figure 4 Fluorescent analogs gangliosides synthesized by a chemical method.

N. Komura *et al*. **2016** 【ref. 61】

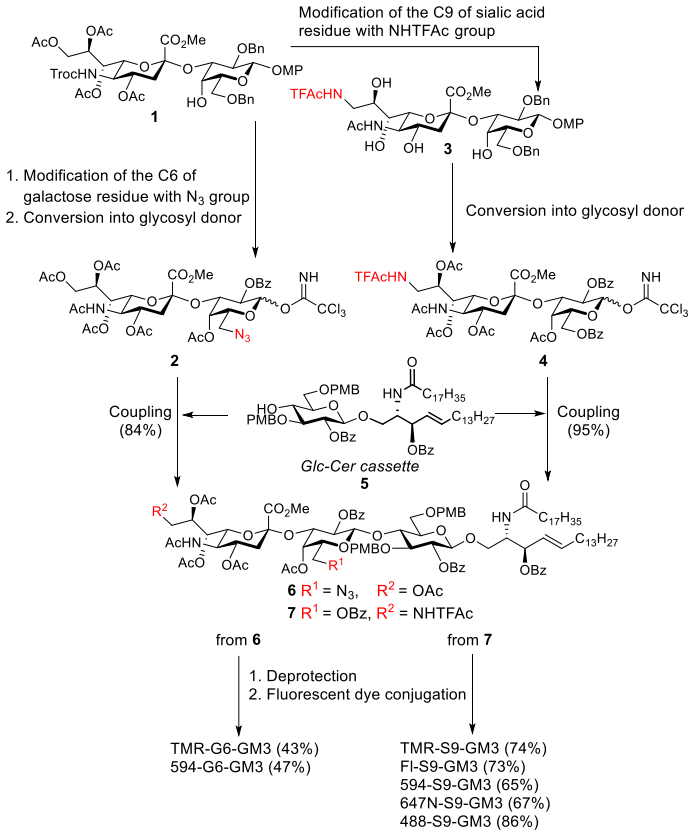

Figure 5 Outline of synthetic routes toward fluorescent analogs of GM3

N. Komura *et al.* **2016** 【ref. 61】

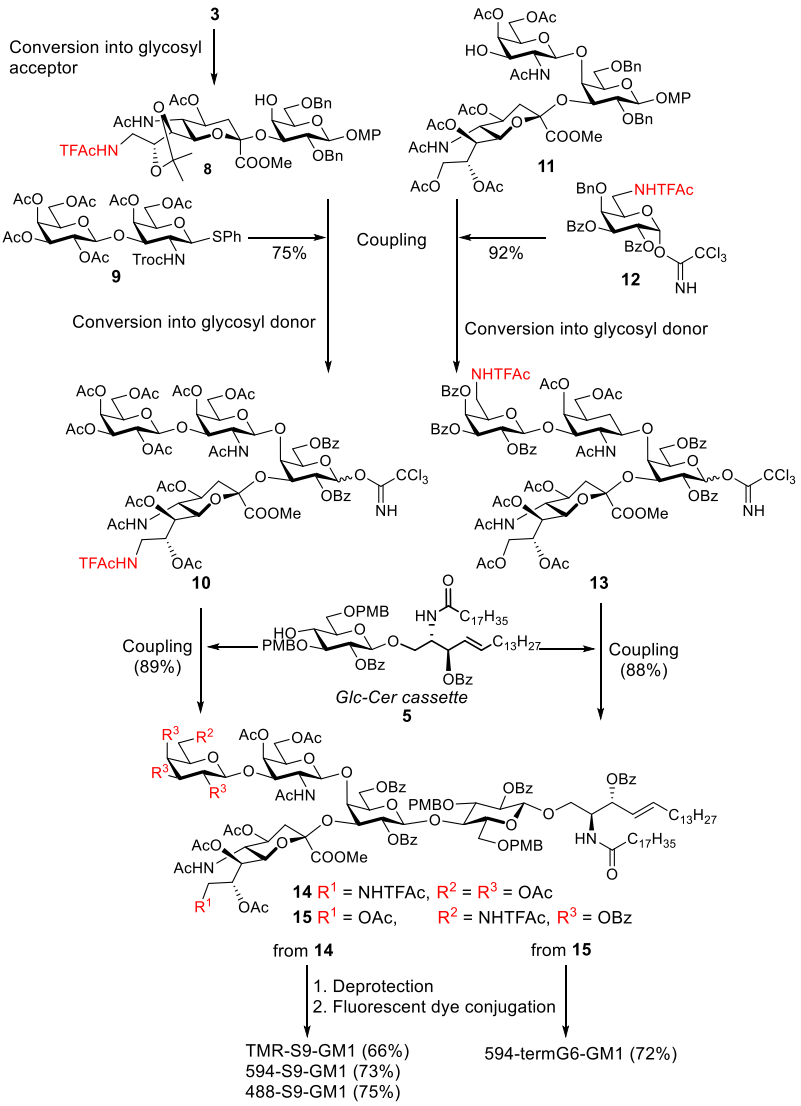

Figure 6 Outline of synthetic routes toward fluorescent analogs of GM1

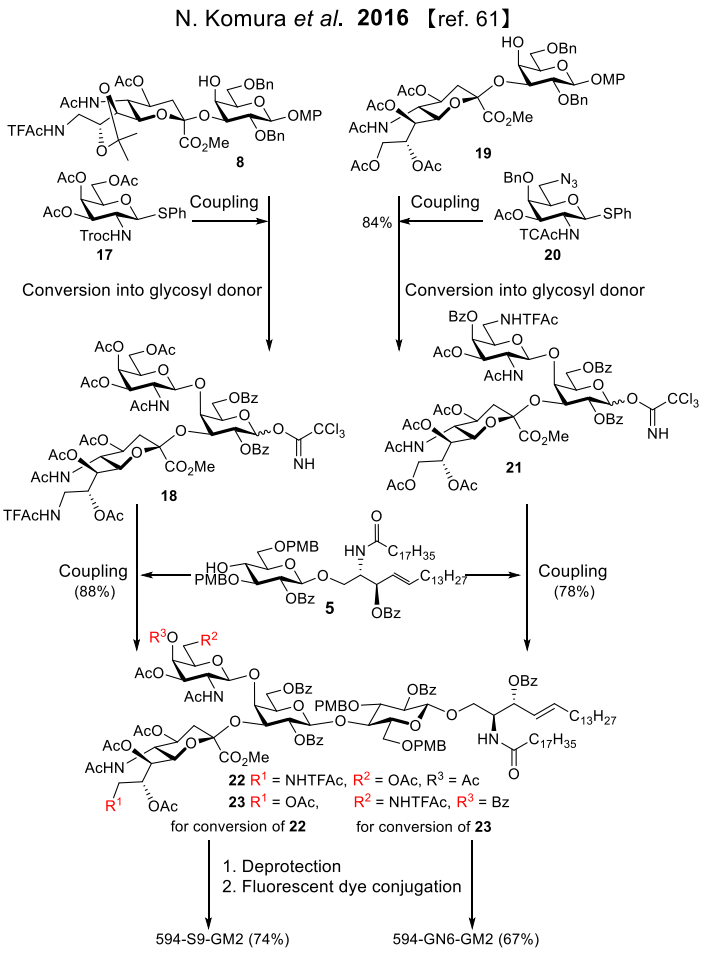

Figure 7 Outline of synthetic routes toward fluorescent analogs of GM2

N. Komura *et al*. **2016** 【ref. 61】

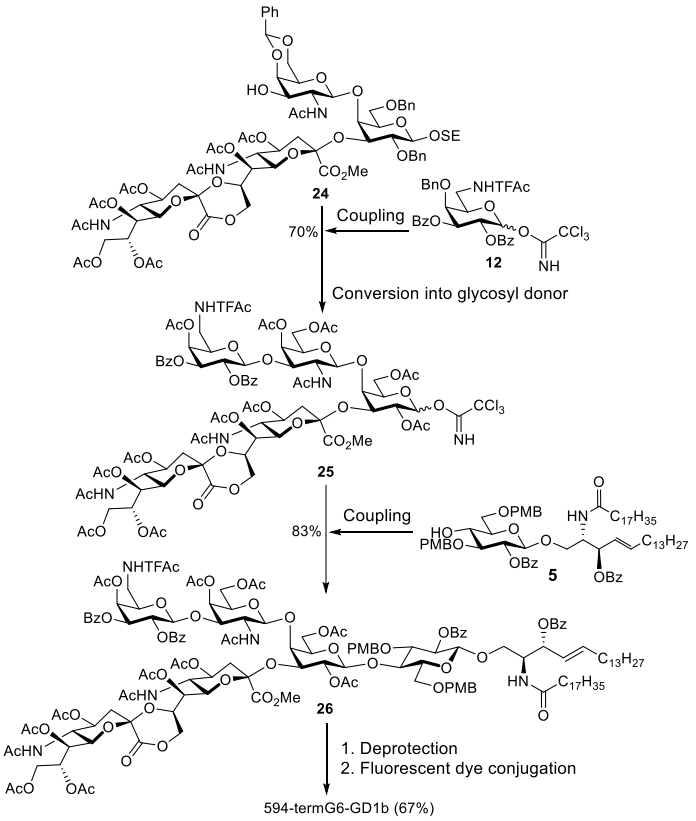

Figure 8 Outline of synthetic routes toward fluorescent analogs of GD1b

a

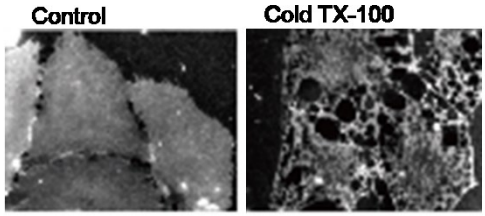

b

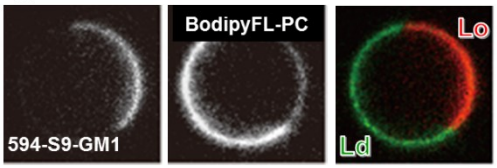

Lo phase: 594-S9-GM1
Ld phase: BodipyFL-PC (non-raft control molecule)

c

Fluorescent gaanglioside	DRM vs. Intact Ratio (mean ± SE)	Lo/Ld Ratio (mean ± SE)
Cy3-CTB	1.2 ±0.08	6.7 ±0.49
BodipyFL-GM1	0.042 ± 0.009	0.62 ± 0.05
TMR-S9-GM1	1.0 ±0.05	1.9 ±0.25
594-S9-GM1	1.1 ±0.08	3.3 ±0.11
488-S9-GM1	1.1 ±0.06	3.0 ±0.23
594-termG6-GM1	1.0 ±0.05	4.7 ±0.35
594-S9-GM2	1.0 ±0.05	4.1 ±0.48
594-GN6-GM2	1.1 ±0.07	4.4 ±0.43
Fl-S9-GM3	1.1 ±0.05	8.8 ±1.5
TMR-S9-GM3	1.0 ±0.10	1.5 ±0.08
594-S9-GM3	1.0 ±0.05	4.0 ±0.14
488-S9-GM3	1.1 ±0.06	4.6 ±0.58
647N-S9-GM3	0.066 ± 0.008	0.26 ± 0.02
TMR-G6-GM3	0.029 ± 0.006	1.7 ±0.14
594-G6-GM3	0.49 ± 0.04	1.7 ±0.09
594-termG6-GD1b	1.0 ±0.04	4.2 ±0.40

Figure 9 Partitioning of fluorescent ganglioside analogs. (a) Analysis for partitioning into DRMs. (b) Analysis for partitioning into Lo- and Ld-like domains in the GPMVs. (c) Results of biophysical evaluation.

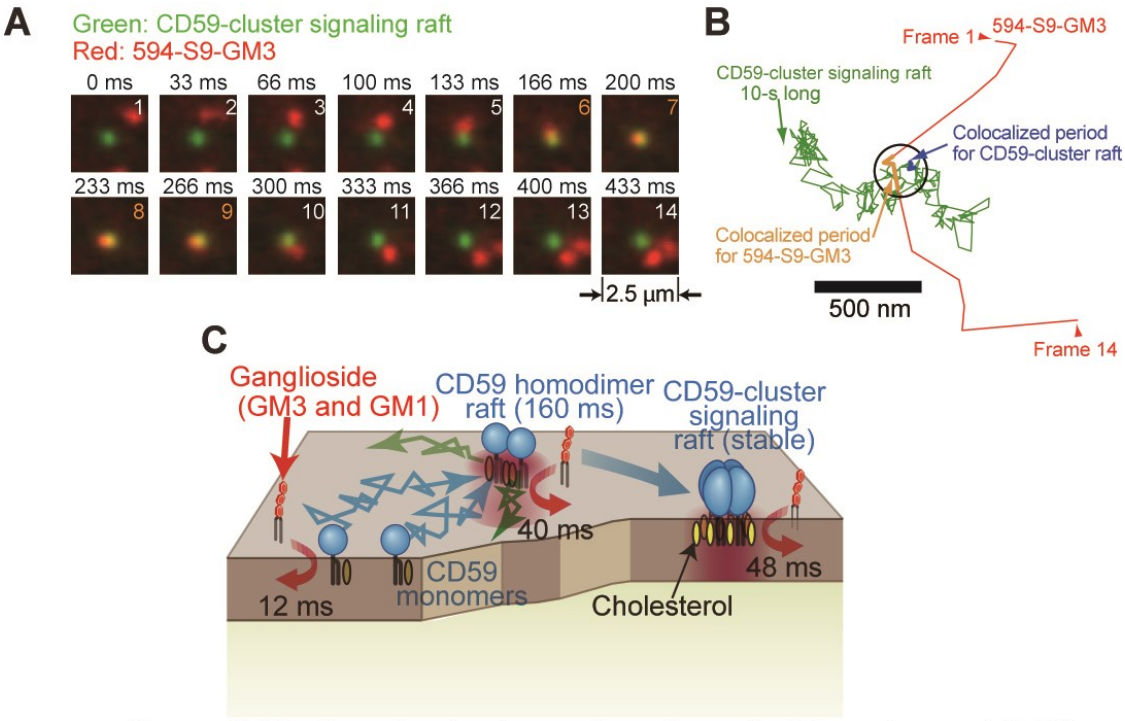

Figure 10 Single-molecule observation of ganglioside probes and CD59